JMEPEG (2012) 21:1003–1007
DOI: 10.1007/s11665-011-9957-5

1059-9495/$19.00

Subcritical Spheroidization of Medium-Carbon 50CrV4 Steel

W.Y. Guo, J. Li, and X.F. Jiang

(Submitted October 29, 2010; in revised form April 9, 2011)

An investigation on subcritical spheroidization anneal of the cold-rolled 50CrV4 steel at 720 °C has been carried out. During spheroidization anneal, the lamellar cementite was gradually broken down and changed to spherical shape. With prolonging of soaking time, the amount of lamellar cementite decreases gradually, and that of the spheroidized cementite particle increases gradually. The relationship of the spheroidization ratio versus soaking time for the steel can be described by a typically sigmoid curve. Additionally, the cold rolling deformation accelerates the breakup of lamellar cementite and the formation of spheroidal cementite particles during spheroidization anneal of the steel. The more severe the deformation is, the more rapidly the spheroidization occurs. From the results of tensile and hardness test, the yield strength, ultimate tensile strength, and hardness decrease and the percentage elongation to failure increases rapidly during the first 2 h of spheroidization. Between 2 and 8 h, the yield strength, ultimate tensile strength, hardness nearly keep a constant, which are independent of the soaking time, whereas the percentage elongation to failure firstly increases and then decreases with prolonging of soaking time.

Keywords 50CrV4 steel, mechanical property, microstructure, spheroidization, subcritical

1. Introduction

The high strength medium-carbon 50CrV4 steel is being used to manufacture the automotive clutch diaphragm, which is a kind of plate-type spring. This steel is usually treated by spheroidization anneal using batch furnace before applying cold forming processes to obtain the spheroidized microstructure with finely distributed spherical cementite particles in a ferrite matrix. The spheroidization treatment is by far the most time-consuming phase of spring manufacture, which causes an increase in the amount of energy utilized in the process, so the reduction of the time for spheroidization leads to major energy saving.

Two spheroidization processes are often applied in industry. One is the intercritical spheroidization, in which the steel is heated above the A_{c1} temperature for approximately 2 h and then slowly cooled below the A_{c1} and held for various periods and subsequently furnace cooled. The other process is the subcritical spheroidization, which consists of heating below the A_{c1} for various times before cooling to room temperature (Ref 1, 2). Work done by O'Brien et al. (Ref 2, 3) confirms that the subcritical process requires much less spheroidization time for medium-carbon steel than the intercritical process. Therefore, subcritical spheroidization process is a promising process for medium-carbon steel for industrial application.

Some articles have been published about the spheroidization anneal of medium-carbon steel (Ref 2-7). However, very little has been written about the details of the high strength medium-carbon 50CrV4 spring steel. Therefore, in this research, a systematic study about subcritical spheroidization anneal of 50CrV4 steel has been performed to quantify the effects of various combinations of cold-rolling reduction ratio as well as annealing time.

2. Experimental

The starting material used in this study is the cold-rolled 50CrV4 steel sheets, of which the thickness is 2.95 and 1.65 mm, and the corresponding reduction ratio is 24 and 58%, respectively. The steel contains 0.543 pct C, 0.23 pct Si, 0.827 pct Mn, 1.012 pct Cr, 0.137 pct V, and 0.019 pct Al with 0.011 pct P and 0.001 pct S. The lower critical temperature (A_{c1}) of the steel is 740 °C and the upper (A_{c3}) is 790 °C.

The rectangular samples with dimension of 300 mm length and 200 mm width were cut from the steel sheets and then subcritically annealed at 720 °C, followed by furnace cooling to room temperature at approximately 10 °C per minute. The spheroidization anneal process was performed in a batch-type high-temperature controlled atmosphere furnace, with temperature measurement accuracy of better than 1 °C. The soaking time was varied from 2 to 8 h, so the changes of microstructure and mechanical properties with time could be studied. Before spheroidization treatment, a reducing 100% H_2 atmosphere was fed into the furnace to avoid the presence of O_2 which may cause a sample surface oxidation during annealing.

Metallographic specimens were prepared according to the standard procedure from the spheroidized samples and

W.Y. Guo, Shanghai Baoyi Can Making Co., Ltd, Shanghai 201908, China; **J. Li**, Research Institute, Baoshan Iron & Steel Co., Ltd, Shanghai 201900, China; and **X.F. Jiang**, School of Materials Science and Engineering, Shanghai Jiao Tong University, Shanghai 200240, China. Contact e-mail: guowenyuan2@yahoo.com.

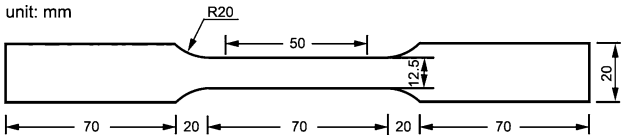

Fig. 1 Schematic diagram of tensile specimen

etched with 4% nital solution. Microstructure observations were carried out in a Hitach 3400 scanning electronic microscope. At least 5 SEM micrographs for each condition were examined to determine the degree of spheroidization using an image analysis program (ImageJ version 1.42). The cementite particles with the aspect ratio less than 3 were considered as spheroidal particles.

Plate-type tensile specimens, as shown in Fig. 1, were machined from the spheroidized samples in parallel to the rolling direction. The tensile test was conducted using a Zwick tensile testing machine at room temperature according to ISO 6892:1998. The test speed is 30 mm/min, which corresponds to a strain rate of 10^{-2}/s. At least three specimens were tested and average values were calculated for each condition. Key parameters obtained from stress-strain curves include yield strength, ultimate tensile strength, and percentage elongation to failure. The Vickers hardness of all specimens was measured at a load of 1 kg. The hardness presented is the average of at least five values.

3. Results and Discussion

The microstructure of the cold-rolled 50CrV4 steel consists of a great deal of pearlite colonies distributed in the ferrite matrix, as shown in Fig. 2. With increasing reduction ratio, the pearlite lamellae are gradually bended and tend to parallel to the rolling direction. The breakup of lamellar cementite at pearlite colony boundaries caused by deformation was observed and it is more severe in the 58% cold-rolled steel.

Figure 3 shows the microstructural evolution of the 24% cold-rolled 50CrV4 steel during spheroidization anneal at 720 °C. After 2 h spheroidization, most of the cementite plates have broken into relatively small pieces or into long narrow ribbons, and a small amount of cementite particles have been observed to form in the microstructure. With prolonging of soaking time, the ribbon-like cementite gradually changed their shapes and became long narrow rods and then broke down into a series of small spheroids. After 8 h spheroidization, the spheroidized cementite particles have distributed all over the ferrite matrix non-uniformly and a considerable amount of remained lamellar cementite still can be observed.

The 58% cold-rolled 50CrV4 steel exhibits similar microstructural evolution during spheroidization anneal at 720 °C, as shown in Fig. 4. Moreover, it can be seen obviously that the breakup of lamellar cementite and the formation of spheroidal cementite are accelerated, and the microstructure after 8 h annealing consists of newly formed uniform spherical cementite particles and a slight amount of cementite lamellae, which demonstrates a well-spheroidized structure.

The spheroidization ratio, denoted as the ratio between volume fraction of the spherical cementite particles and the total volume fraction of all cementite particles, which was measured by ImageJ from SEM images enhanced to show only

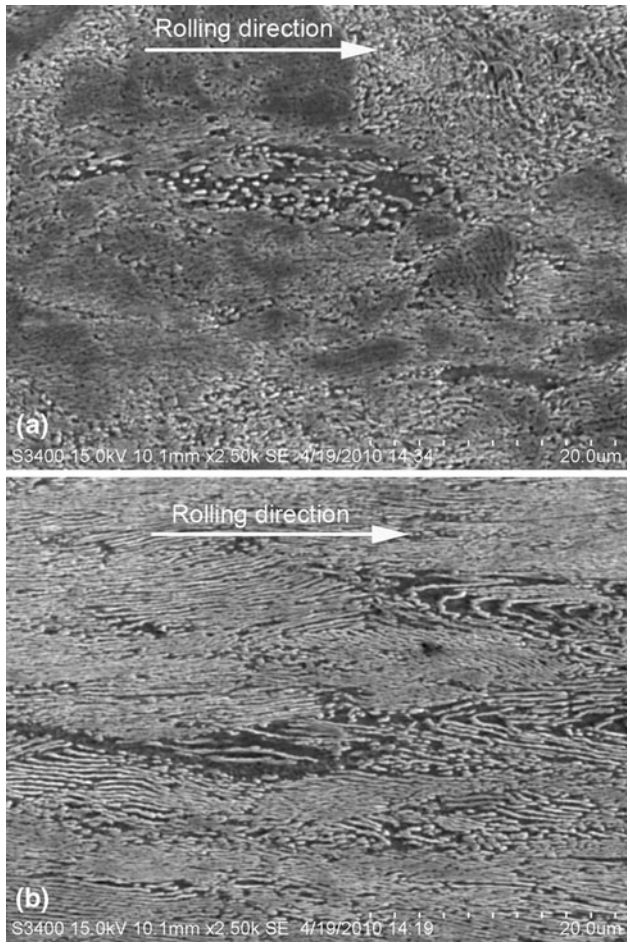

Fig. 2 Microstructure of the cold-rolled 50CrV4 steel with reduction ratio of 24% (a) and 58% (b)

the carbide particles, indicating the effectiveness of an annealing process, as show in Fig. 5. The relationship between the spheroidization ratio and the soaking time at 720 °C for the cold-rolled 50CrV4 steel is plotted in Fig. 6. It can be seen that the relationship of the spheroidization ratio versus soaking time for the cold-rolled steel can be described by a typically sigmoid curve. The spheroidization ratio increases slowly at the initial stage of the annealing and then rapidly when soaking time is over 2 h. However, the increase of spheroidization ratio was observed to gradually slow down when soaking time is over 6 h.

From the results of tensile test, the yield strength and ultimate tensile strength were found to decrease and the percentage elongation to failure increases rapidly during the first 2 h of spheroidization. Between 2 and 8 h, the yield strength and ultimate tensile strength nearly keep a constant, which are independent of the soaking time, whereas the percentage elongation to failure first increases and then decreases with prolonging of soaking time, as seen in Fig. 7. The 58% cold-rolled steel always shows lower strength and better ductility than the 24% cold-rolled one at the same soaking time. This is may be due to the homogeneously distributed carbides inside the 58% cold-rolled steel.

Figure 8 shows the variation of hardness (Hv) with soaking time at 720 °C for 50CrV4 steel. It is clear from this figure that the difference in hardness between the two samples is not

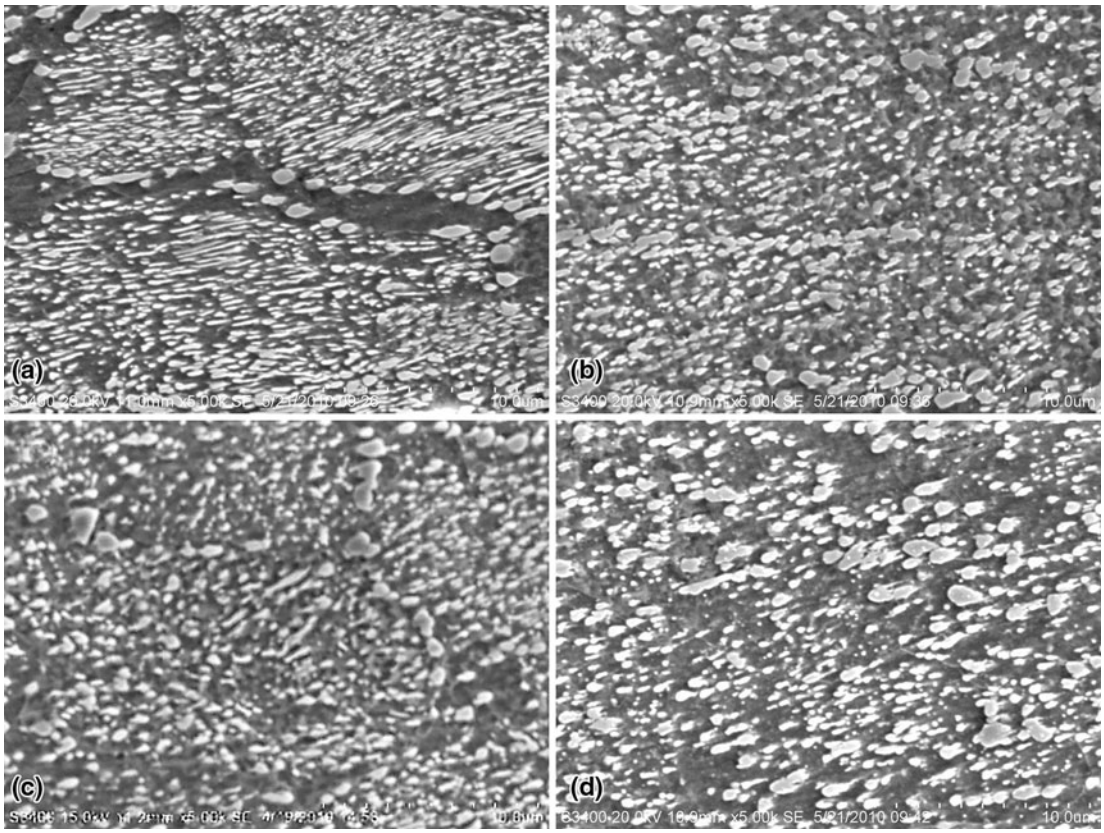

Fig. 3 Microstructural evolution of the 24% cold-rolled 50CrV4 steel annealed at 720 °C for 2 h (a), 4 h (b), 6 h (c), and 8 h (d)

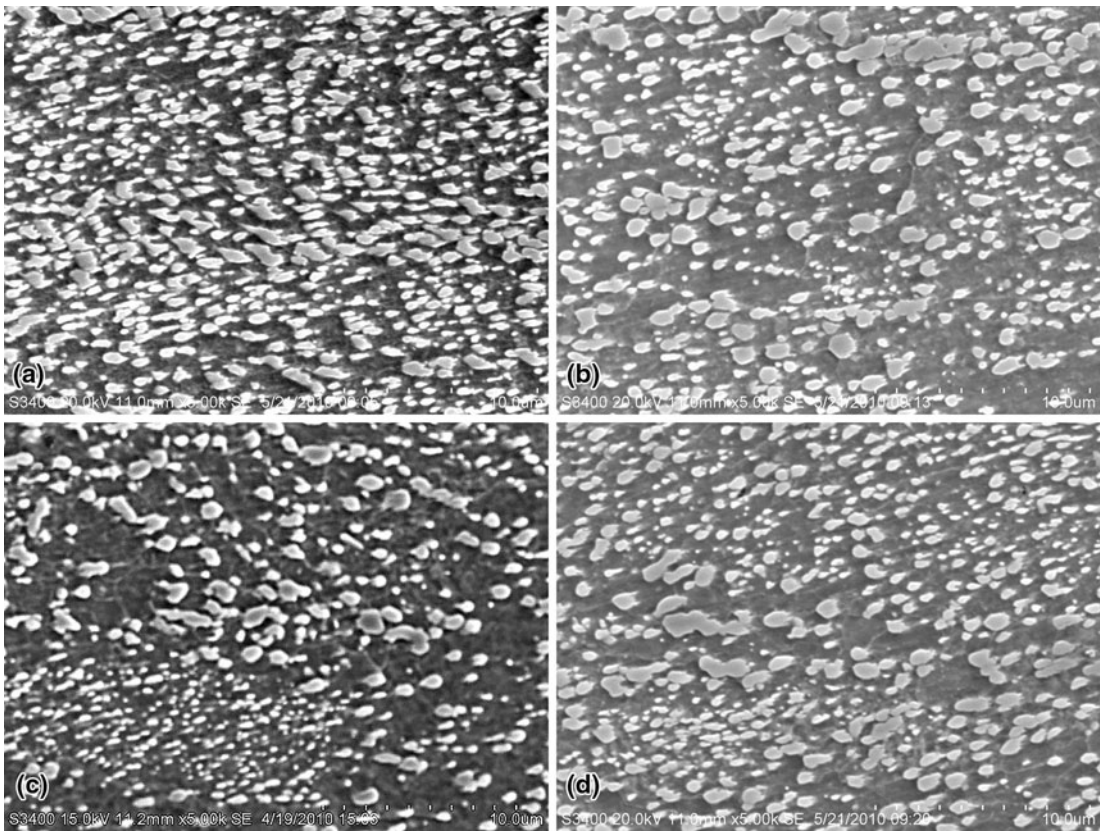

Fig. 4 Microstructural evolution of the 58% cold-rolled 50CrV4 steel annealed at 720 °C for 2 h (a), 4 h (b), 6 h (c), and 8 h (d)

Fig. 5 Enhanced image showing only the areas of carbide particles in the 24% cold-rolled 50CrV4 steel after 6 h annealing at 720 °C

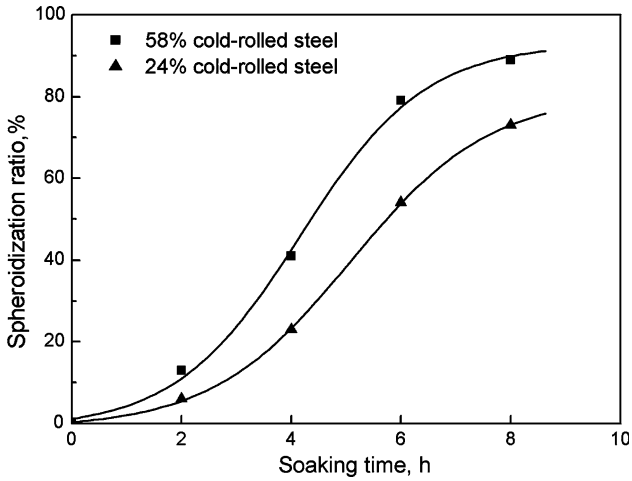

Fig. 6 Relationship of the spheroidization ratio versus soaking time for 50CrV4 steel

significant. In the cold-rolled state prior to heat treatment, the steel shows higher hardness. During spheroidization anneal, the hardness drops sharply at the first 2 h. But between 2 and 8 h of soaking time, hardness remains nearly constant.

Tian et al. (Ref 8) reported that the interlamellar spacing and the density of faults are the main factors that play important roles in the rate of spheroidization. The reduction in interlamellar spacing should increase the number of plates per unit area as well as the number of Fe-Fe_3C interfaces, thereby increase the rate of spheroidization by shortening diffusion path for iron and carbon atoms (Ref 9-12).

The sigmoidal kinetics of the spheroidization ratio versus soaking time probably related to spheroidization process. Spheroidization initiates and develops from the lamellar faults like subboundaries, holes, and fissures. The growth of boundaries groove or the expansion of holes and fissures result in the break-up of cementite lamellae into smaller segments whose sharp edges became subsequently smoothened by the diffusion of iron and carbon atoms (Ref 13, 14). In the first 2 h of spheroidization, the groove is growing, the holes and fissures are expanding, and little cementite lamellae can break into smaller segments. In this time only smaller segments caused by deformation change their shapes to a series of small spheroids,

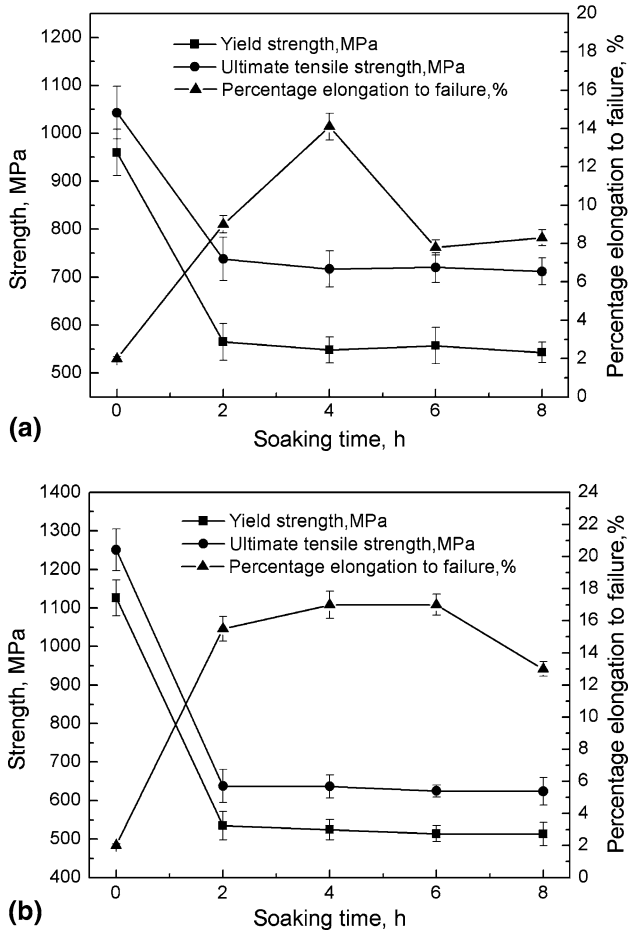

Fig. 7 Mechanical properties of 50CrV4 steel with reduction ratio of 24% (a) and 58% (b) during spheroidization

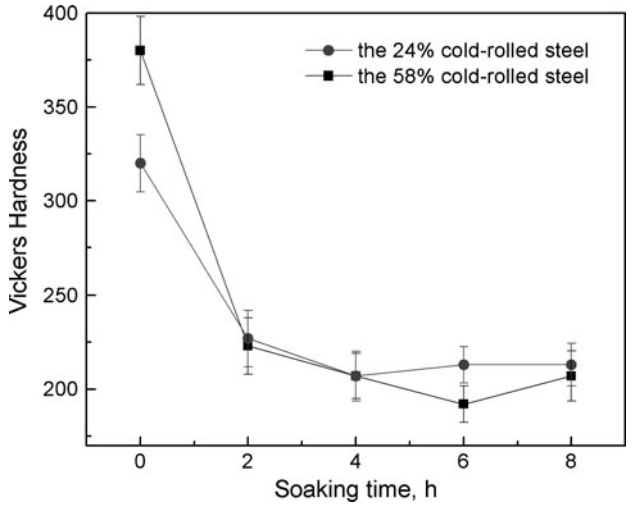

Fig. 8 Hardness change during spheroidization of 50CrV4 steel

so the speroidization ratio increases slowly. When annealing time is over 2 h, large amount of cementite lamellae break into smaller segments, and whose sharp edges became subsequently smoothened, which leads to the rapid increase in speroidization ratio. When annealing time is over 6 h, no more cementite lamellae can be break up, and there are only the diffusion of

iron and carbon atoms, therefore, the increase of speroidization ratio was observed to gradually slow down.

Plastic deformation favors spheroidization since it is expected to cause reduction of interlamellar spacing and introduce large amounts of dislocations into cementite lamellae, and the movement and accumulation of dislocations led to the occurrence of subboundaries, holes, and fissures. The reduction of interlamellar spacing and the density of faults increase with the reduction ratio of the steel, which may lead to possible fracture of an increasing number of cementite particles, so the enhanced spheroidization of cementite was observed in the 58% cold-rolled steel.

The higher strength (including yield strength and ultimate tensile strength), the lower percentage elongation to failure, and the higher hardness of the cold-rolled steel are mainly due to the presence of finer microconstituents of ferrite and pearlite and the work-hardening effect. The marked decrease of strength and hardness and increase of percentage elongation to failure in the first 2 h of spheroidization can be attributed to the release of internal stress, the recrystallization of the deformed ferrite matrix, and the elimination of lamellar pearlite and the generation of cementite spheroids in the microstructure. The stable value of the strength and the hardness of the steel between 2 and 8 h of soaking time implies that the work-hardening effect has been eliminated and the recrystallization of the deformed ferrite matrix has finished, whereas the degree of spheroidization, size, and spatial distribution of the spheroidal cementite have little effect on the strength and the hardness.

4. Conclusion

The evolution of the microstructure during the spheroidization anneals and its effect on mechanical properties of the cold-rolled 50CrV4 steel was investigated and the results can be summarized as follows:

(1) Cold rolling deformation is effective in accelerating the breakup of lamellar cementite and the formation of spheroidal cementite particles for the steel. The more severe the deformation is, the more rapidly the spheroidization occurs.
(2) Spheroidization of the cold-rolled steel has been characterized by the percent of carbide particles with aspect ratio less than 3. The relationship of the spheroidization ratio versus soaking time for the cold-rolled steel can be described by a typically sigmoid curve.
(3) Soaking time initially decreases the strength of the steel but has little effect on the strength and the hardness of the steel between 2 and 8 h.

Acknowledgments

The study was supported by The Shanghai Postdoctoral Sustentation Fund under the contract No. 09R21420300. The authors gratefully acknowledge Dr. S. H. Xiang and Sr. Engineer H.M. Li, Research Institute, Baoshan Iron & Steel Co., Ltd., for the use of a vacuum furnace and laboratory facilities.

References

1. N.V. Luzginova, L. Zhao, and J. Sietsma, The Cementite Spheroidization Process in High-Carbon Steels with Different Chromium Contents, *Metall. Mater. Trans. A*, 2008, **39A**, p 513–521
2. J.M. O'Brien and W.F. Hosford, Spheroidization Cycles for Medium Carbon Steels, *Metall. Mater. Trans. A*, 2002, **33A**, p 1255–1261
3. J.M. O'Brien and W.F. Hosford, Spheroidizing of Medium Carbon Steels, *19th ASM Heat Treating Society Conference,* S.J. Medea, G.D. Pfaffmann, Eds., Materials Park, Ohio, ASM, 2000, p 638–645
4. Y. Kanetsuki, M. Katsumata, and T. Inoue, Relation Between Fine Ferrite-Pearlite Microstructure Produced by Controlled Rolling and Cooling and the Subsequent Rapid Spheroidization of Medium Carbon Steel, *J. Iron Steel Inst. Jpn.*, 1990, **76**, p 73–80
5. J.M. O'Brien and W.F. Hosford, Spheroidization of Medium-Carbon Steels, *J. Mater. Eng. Perform.*, 1997, **6**, p 69–72
6. E. Karadeniz, Influence of Different Initial Microstructure on the Process of Spheroidization in Cold Forging, *Mater. Des.*, 2008, **29**, p 251–256
7. U.G. Gang, J.C. Lee, and W.J. Nam, Effect of Prior Microstructure on the Behavior of Cementite Particles During Subcritical Annealing of Medium Carbon Steels, *Met. Mater. Int.*, 2009, **15**, p 719–725
8. V.V. Shkatov, A.P. Chernyshev, and V.I. Lizunov, Kinetics of Pearlite Spheroidization in Carbon Steel, *Phys. Met. Metall.*, 1990, **70**, p 116–121
9. Ö.E. Atasoy and S. Özbilen, Pearlite Pheroidization, *J. Mater. Sci.*, 1989, **24**, p 281–287
10. L.E. Samuels, *Optical Microscopy of Carbon Steels*, ASM, Metals Park, OH, 1980, p 225–229
11. K.W. Andrews, Empirical Formulae for the Calculation of Some Transformation Temperatures, *J. Iron Steel Inst.*, 1965, **203**, p 721–727
12. Y.L. Tian and R.W. Kraft, Kinetics of Pearlite Spheroidization, *Met. Trans. A*, 1987, **18A**, p 1359–1369
13. Y.L. Tian and R.W. Kraft, Mechanisms of Pearlite Spheroidization, *Met. Trans. A*, 1987, **18A**, p 1403–1414
14. S.E. Nam and D.N. Lee, Accelerated Spheroidization of Cementite in High-Carbon Steel Wires by Drawing at Elevated Temperatures, *J. Mater. Sci.*, 1987, **22**, p 2319–2326